Research Square

Preprints are preliminary reports that have not undergone peer review.
They should not be considered conclusive, used to inform clinical practice,
or referenced by the media as validated information.

Discovery of QTLs Controlling Flavor Compounds in a Sweetpotato Mapping Population

Modesta Abugu
Department of Horticultural Science, North Carolina State University
Gabriel Siqueira Gesteira
Bioinformatics Research Center, North Carolina State University
Suzanne Johanningsmeier
USDA-ARS, Food Science and Market Quality and Handling Research Unit, 322 Schaub Hall, Box 7624, North Carolina State University
Marcelo Mollinari
Bioinformatics Research Center, North Carolina State University
Bode Olukolu
Department of Entomology and Plant Pathology, University of Tennessee
Ken V. Pecota
Department of Horticultural Science, North Carolina State University
Massimo Iorizzo
Plants for Human Health Institute, Department of Horticultural Science, North Carolina State University
G. Craig Yencho
Craig_Yencho@ncsu.edu

Department of Horticultural Science, North Carolina State University

Research Article

Keywords: sensory attributes, volatile organic compound, candidate genes, sweet potato, Ipomoea batatas

Posted Date: June 19th, 2026

DOI: https://doi.org/10.21203/rs.3.rs-9905073/v1

License: This work is licensed under a Creative Commons Attribution 4.0 International License.
Read Full License

Additional Declarations: No competing interests reported.

Abstract

Flavor is an important trait influencing consumer preference for sweetpotato, yet little is known about the genetic mechanisms controlling the volatile organic compounds (VOCs) that may contribute to the flavor of cooked roots. In this study, a biparental mapping population consisting of 362 genotypes was used to perform the first genetic study of VOCs in cooked sweetpotato. VOC identification was carried out using headspace solid-phase microextraction and 2-dimensional gas chromatography coupled to time-of-flight mass spectrometry. In total, 176 VOCs were analyzed, including 27 compounds which were previously identified as predictors of different flavor attributes in sweetpotato, and 14 compounds whose identities remain unknown. A high-density phased genetic linkage map including 14,364 single nucleotide polymorphism markers was used for quantitative trait loci (QTL) mapping. A total of 86 QTLs were identified, including 2 monoterpenes and 2 apocarotenoids that have been associated with a “cooked carrot” flavor in sweetpotato. No QTLs were observed for VOCs important in the prediction of “sweetpotato” and “caramel” flavor attributes, suggesting that substrates for those VOCs vary across the population, and may be influenced by multiple interacting factors. This study provides a foundation for the genetic dissection of flavor in sweetpotato and offers new opportunities for incorporating desirable VOC profiles into breeding programs to enhance consumer appeal of new varieties.

1.0 Introduction

Sweetpotato *(Ipomoea batatas)* is a specialty crop whose production and consumption has doubled over the past decade, driven by effective marketing campaigns and consumers' growing recognition of its nutritional properties (George et al., 2024). Sweetpotatoes are a rich source of bioactive and antioxidant compounds, and their unique flesh colors, textures, aromas and flavors make them suitable to various culinary applications. With increasing demand, improving sweetpotato flavor has become both a breeding target and a long-term goal for the sweetpotato industry.

Flavor is a major driver of consumer preference for cooked sweetpotatoes (Kays 2005). It is perceived through a complex process involving the interaction of multiple sensory systems (Wang & Kays, 2001). During cooking, sweetpotato storage roots generate a variety of volatile organic compounds (VOCs). When chewing, the VOCs released from the food matrix travel to the olfactory receptors in the nose, where they are perceived collectively as flavor (Chen et al., 2023).

Despite its importance to consumers, the genetic basis of sweetpotato flavor is still poorly understood. This knowledge gap is largely due to the expensive and time-consuming methods used to evaluate flavor (sensory analysis) and VOC profiles (e.g. Gas Chromatography–Mass Spectrometry- GC-MS), as well as various other factors, such as post-harvest curing, genotypes and cooking methods, that influence the composition and stability of flavor compounds (Wang et al., 1996, Wang and Kays 2001, Shen et al., 2024).

Cooked sweetpotato VOCs can arise from several mechanisms, including the degradation of carbohydrates and amino acids during the Maillard Reaction (MR), as well as oxidation of fatty acids,

carotenoids and terpenes (Kays and Wang 2000). Over 400 VOCs were identified across 22 studies in cooked sweetpotato using GC-MS, with a few of them reported to be odor active (Abugu et al. 2025a). Most recently, a sweetpotato biparental mapping population was used to determine the volatile compounds associated with 10 flavor attributes (including “sweetpotato”, “caramel”, “cooked carrot”, “baked potato”, “roasted chestnut”, “earthy”, “cooked green”) (Abugu et al., 2025b). These studies established links between VOCs and flavor perception, opening opportunities to investigate the genetic mechanisms controlling VOC formation to enable DNA-based strategies to select sweetpotato varieties with desirable flavor profiles.

Recent advances in sweetpotato genomics have provided new opportunities for quantitative trait loci (QTL) analyses and DNA marker-assisted breeding (Mollinari et al., 2020; Wadl et al., 2018; Wu et al., 2018; Da Silva Pereira et al., 2020). QTL analysis has been used to study the genetic architecture of traits such as root knot nematode resistance (Fraher et al., 2024; Oloka et al., 2021), β-Carotene (BC) content (Cervantes-Flores et al., 2011; Gemenet et al., 2020; Haque et al., 2020; Kinczyk, 2019; Yada et al., 2017; Yu et al., 2014), anthocyanin content (Haque et al., 2020), and sugar content (Kinczyk 2019) in sweetpotato. Studies in other crops, including tomato (Martina et al., 2021), citrus (Yu et al., 2017), apples (Costa et al., 2013; Yang et al., 2023) peanuts (Zhang et al., 2023), and beans (Bassett et al., 2021), have identified QTLs associated with flavor traits, revealing the genetic architecture of key VOCs. However, no study has identified QTLs for VOCs in sweetpotato.

In this study, we utilized a high-resolution phased genetic linkage map alongside phenotypes for VOC profiles from a biparental population to perform the first QTL study for key flavor compounds in sweetpotato.” By identifying QTLs for key flavor-associated compounds, this study lays the groundwork for developing molecular markers to screen and select for consumer-preferred flavors in sweetpotato, while providing a framework for future investigations into VOCs influenced by both genetic and environmental factors.

2.0 Materials and Methods

2.1 Plant Material

The “NCDM04-001” x “Covington” (DC) mapping population, developed by the NCSU sweetpotato breeding program, comprised of 416 progenies (Kinczyk 2019), was used as plant materials in this study. NCDM04-001 is a high dry matter, low β-carotene (BC), low reducing sugar breeding line, while Covington is a low dry matter, high BC, moderate reducing sugar cultivar (Yencho et al., 2006). The resulting DC progenies have been reported to transgressively segregate for starch, BC and sugars (Kinczyk 2019); and exhibit wide variation in volatile profiles (Abugu et al 2025b). Since its development in 2017, the population has been maintained both as greenhouse plants in disease-free conditions and as storage roots propagated from vegetative cuttings in the field. In the summer 2023, all 416 DC genotypes were planted from vegetative 25–30 cm long tip cuttings obtained from storage roots planted (bedded) in 40.0 cm x 40.0 cm x 12.7 cm plant trays (AFLAT5, 0.48cm bottom mesh, Anderson Pots, Portland, OR) in

a plastic tunnel house. Experimental plots consisted of six plant plots with 28 cm between plants and 1.06 m between ridged rows. A purple-colored clone was planted between plots to maintain consistent growth and enable easy plot identification. The growing season for cultivars was 132 days after planting and harvest was done on October 19th, 2023. Storage roots were cured after harvest for 7 days at 80^{O}F and 85% RH and stored in the breeding program's specialized sweetpotato storage facility, in Clinton NC at 58^{O}F and 85% RH. As of 1st February 2024, roots had been 98 days in storage.

2.2 Volatile Compound Profiling

Volatile compound profiling was done for the harvested roots using the sample preparation method reported in Zhang et al., 2021 with slight modifications. For each genotype, 6 roots were used to obtain core samples using a 5 mm metal cork borer (Humboldt, H-9665; Schiller Park, IL, USA). The core samples were flash-frozen in liquid nitrogen and milled into a uniform puree using a Retsch MM 400 mixer mill (Retsch Technology, Haan, DE). Approximately 500 mg of puree was transferred into headspace vials (Wheaton Microliter cat#16-1000), mixed with 1 mL saturated NaCl and 10 µL of the internal standard (0.005 ng/µl ethylbenzene- d-10 solution), and sealed. Three technical replicates from a subset of samples were prepared to assess reproducibility. Samples were placed in a Gerstel MPS2 refrigerated autosampler (Model CTC Analytics (Switzerland), LEAP Technologies, Carrboro, NC, USA.) and held at 4°C for analysis. The samples were heated directly in the sealed vials to mimic oven-cooked sweetpotato conditions, achieved by incubating them at 80°C for 30 min. Following this heating step, VOCs were extracted under the same temperature (80°C) for an additional 30 min with a PDMS-Carboxen-DVB solid-phase microextraction (SPME) fiber while agitating at 500 rpm (5s on, 2s off). The extracted sweetpotato volatile compounds were separated using a two-dimensional gas chromatograph (GC × GC) attached to a 4D high-resolution time of flight mass spectrometer (ToFMS) (LECO Corporation, St Joseph, MI, USA). Volatile compounds were desorbed in the GC inlet (Restek, Bellefonte) at 250°C for 15 min operated in pulsed spitless mode with a pulse pressure of 255 kPa for 1 min. The GC × GC primary oven was maintained at 40°C for 2 min and then increased at 5°C/min to 140°C. The temperature ramp then increased to 10°C/min to 250°C and oven was held at 250°C for 3 min. The secondary oven was run at an offset temperature of 10°C above the temperature of the primary oven. The modulator offset was 30°C with a 4 s 2nd-dimension separation time and a 0.80 s hot pulse time. After separation, volatile compounds were detected using an electron ionization of − 70 eV; a source temperature of 200°C; stored mass range: 25–500 µ; and an acquisition rate: 200 spectra/s.

2.2.1 Chromatographic Data Processing and Semi-quantitative Analysis of Flavor- associated VOCs

Following the exclusion of genotypes lost during harvest or storage and samples with poor-quality chromatograms, 362 samples were retained for data processing. A three-level data processing approach was used to identify the VOCs used in this study. Firstly, a peak find method was applied to identify all peaks in the 362 genotypes using a ChromaTOF software (LECO Corporation, St. Joseph, MI). Peaks were detected at a signal-to-noise ratio ≥ 10 and matched against the NIST 20 library with similarity ≥ 800

and peak width = 0.06s. Secondly, an untargeted analysis and chromatogram alignment were performed using LECO ChromaTOF Tile (v.1.01, LECO Corporation, St. Joseph, MI). Sample classes included 362 genotypes (sample class) and 74 blanks, with a tile size of 10 modulations (8 s) × 45 spectra (300 ms). Peaks were identified using the same parameters as the peak find method above with RI deviation ≤ 50. Tile hits were ranked by F-ratio ≥ 20, and features more abundant in blanks were removed as artifacts. The resulting annotations (225 VOCs) were validated by manual inspection against ChromaTOF peak tables, comparing retention times, retention indices, and mass spectra. A total of 149 curated VOCs were retained for further analysis. Finally, a target analyte find method was applied for the targeted identification of flavor-associated compounds previously reported in the DC population (Abugu et al., 2025b). From that study, 27 compounds whose identities were confirmed against authentic standards were selected for inclusion in the final VOC list. Analyte find parameters were set using the retention times in the first and second dimensions and key mass fragments of selected compounds.

All identified VOCs were collated for subsequent data analysis. Least squares mean (LS-means) regression was used to identify the differentiating VOCs among genotypes and a Pearson correlation was subsequently performed to assess relationships among these compounds. To evaluate the distribution of phenotypic variation among progeny, frequency histograms were constructed for each differentiating VOC. These differentiating VOCs were then used for QTL mapping. All statistical and data analyses were conducted using JMP Pro 15.2.0 (SAS Institute Inc., Chicago, IL, USA) and R 'stats' package (R Core Team, 2022), 'ggcorrplot' package (version 0.1.4.1) (Kassambara, 2016), 'factoextra' (version 1.0.7) (Kassambara & Mundt, 2016) and 'ggplot2' package (version 3.4.4) (Wickham et al., 2007).

2.3 QTL Analysis

The construction of the DC genetic linkage map was described by Kinczyk (2019). In summary, high-quality GBS data was generated using a GBS protocol adapted for polyploids (GBSpoly, Rickman et al. 2025). Sequence reads were aligned against the I. *trifida* reference genome, and variants and genotypes were called using TASSEL4-Poly and SuperMASSA (Serang et al., 2012, Pereira et al., 2018). Genotype dosages were filtered for quality control attributes, and pairwise recombination fractions were calculated and used for grouping and ordering of markers within chromosomes. Final linkage phases and recombination fractions were jointly re-estimated for the 15 sweetpotato's linkage groups (LG) using a multi-point hidden Markov model (HMM, Mollinari & Garcia, 2019), and final genotype probability distributions used as input for the QTL mapping step.

The resulting high-resolution phased genetic linkage map was based on 14,367 SNP markers distributed among 15 LGs, covering 2,727.1cM of the hexaploid sweetpotato genome. The distribution of dosage combinations in the parents NCDM04-001 and Covington was composed by 51.5% of simplex markers (present in a single copy in one parent and absent in the other,denoted as 0–1, 1 – 0), representing the most abundant form of SNPs in the sweetpotato genome. The average length of the linkage groups was 181.8 cM, with the longest being LG 1 at 243.0 cM, and the shortest being LG 8 at 120.5 cM. Final HMM-based conditional genotype probabilities were calculated and used as input for the QTL mapping step.

The QTLpoly software v. 0.2.4 (https://gabrielgesteira.github.io/QTLpoly/), which provides a random-effect multiple interval mapping framework for QTL mapping in polyploids (Pereira et al., 2020), was used to detect significant QTL of all differentiating VOCs. The conditional genotype probabilities obtained from the genetic linkage map were calculated every 1 cM and used as the source of genetic variation. The VOC peak areas were transformed using a $\log_{10}$ function and used as the phenotypic information in the QTL mapping procedure. Briefly, the procedure searched for putative QTL at every position along the genome based on a stepwise approach, where variance components are tested using score statistics (Qu et al., 2013). First, a null-QTL score distribution was built based on a resampling method with 1000 iterations. The 2th and 5th percentiles of this distribution were used to determine the p-value thresholds for the forward search and backward elimination in the QTL search algorithm. The stepwise procedure followed, where a forward search was used to add one QTL at a time under a less conservative threshold ($p < 0.0006$), followed by a backward elimination procedure where each QTL was tested against a more conservative threshold ($p < 0.0001$). In the backward elimination process, QTLs that fell below the significance threshold or those whose positions changed were dropped from the model. These procedures were repeated until model stabilization, where no QTL was added nor dropped from the model. Based on the final QTL model for each VOC, QTL positions were refined, and their effects jointly estimated, along with associated variance components and heritabilities.

3.0 Results

3.1 Phenotypic Variation of Volatile Compounds in the DC population

This study measured volatile compound profiles in the DC mapping population over one growing season. A total of 176 VOCs were identified, all of which showed sufficient variation among genotypes to differentiate them in least squares regression. The 176 differentiating VOCs were categorized according to their likely mechanisms of formation. Sesquiterpenes were the most abundant class (26%), followed by monoterpenes (19%) and compounds derived from the fatty acid oxidation (14%). Compounds with uncharacterized synthetic mechanisms accounted for 13% of all VOCs, while those likely derived from the Maillard reaction, Strecker degradation and BC degradation comprised 8%, 5% and 3% respectively (Fig S1).

Frequency histograms were generated to evaluate the phenotypic variation among progeny for the differentiating VOCs (Fig S2). Out of the 176 volatile compounds analyzed, 23 (~ 13%) exhibited a likely transgressive segregation pattern, with progeny showing values beyond the range of both parental lines. The distribution patterns varied across compounds, with some VOCs exhibiting highly skewed symmetrical distributions while others showed a bi-modal distribution. For example, several compounds, including 1,2-dihydrolinalool, 1-pentanol, and acetoin, exhibited more symmetrical distributions, consistent with polygenic control and additive genetic effects. A separate group of compounds, (including (E)-2-heptenal, β -cubebene, (-)-; cyperene, (+)-(E)-calamenene, 1-(4-methoxyphenyl)-1-

pentanone, 1-pentanol, 2-butanone, 2-butenal) displayed bimodal distributions which aligns with simple genetic inheritance based on Mendelian segregation. While a few other compounds such as methyl alcohol, 2-carene, and limonene displayed irregular distributions. These distribution patterns indicated complex VOCs biosynthetic pathways or other potential environmental interactions. Furthermore, the frequency histogram of 27 flavor-associated compounds was evaluated (Fig. 1). With the exception of seven compounds (β-myrcene, β-elemene, D- limonene, isobutylalcohol, hexanal, α-terpinine and 1-phenylbutane), most of these flavor-associated compounds displayed a left skewed distribution pattern, showing that most progenies had high levels of the compound, while a few had very low levels (Fig. 1). This further supports the complexity of the VOC traits. Overall, the segregation and diversity of distribution shapes across compounds reveals the underlying heterogeneity in the population and confirms the suitability of these VOCs for QTL mapping and downstream genetic dissection.

3.2 Correlation Analysis for Differentiating and Flavor-Associated VOCs in DC Population

Correlation analysis among the 176 differentiating VOCs revealed that several groups of compounds from shared pathways exhibited similar correlation patterns. For example, 39 sesquiterpenes were significantly positively correlated ($p < 0.01$) with each other and were grouped together in the correlation heatmap (Table S3). The strongest correlations ($r \geq 0.80$) were observed between the following pairs: (-)-germacrene D and β-copaene, aciphyllene and 6,9-guaiadene, rotundene and cypera-2,4-diene, aristolediene and (Z)-calamenene, and β-panasinsene and aristolediene. A similar correlation pattern was observed among the monoterpenes, where the strongest positive correlations occurred between isomers of the same compound. For example, (Z)-linalool oxide and (E)-linalool oxide ($r = 0.98$), 1,2-dihydrolinalool and dihydrolinalool ($r = 0.98$), β-ocimene and allo-ocimene ($r = 0.80$). Additionally, other monoterpenes including (Z)-linalool oxide and 1,2-dihydrolinalool; pinene-7-one and β-ocimene also showed positive correlations ($r \geq 0.71$). Strong positive correlations were also observed among certain apocarotenoids and most monoterpenes e.g α-cyclocitral and carvacrol ($r = 0.89$); dihydro-β-ionone and carvacrol ($r = 0.72$), dihydro-β-ionone and α-ionone ($r = 0.83$). Most compounds derived from Malliard reaction (MR), Strecker degradation (SD), and fatty acid oxidation (FAO) exhibited weak or inconsistent correlations, both within each group and among the different groups. This suggests that their formation is largely independent, reflecting variation in substrate availability across population, and the complex, multi-step nature of these reactions which occur during cooking.

Similarly, a correlation heatmap of the 27 flavor- associated compounds in the DC sweetpotato population (Abugu et al., 2025b; Table S7) revealed predominantly weak or negligible relationships, with only a few notable positive associations (Fig. 2). The strongest positive correlations were observed between (trans)-rose oxide and nerol oxide ($r = 0.81$, $p < 0.01$), two monoterpenes which have been associated with roasted chestnut and earthy flavor notes, respectively. Moderate positive correlations ($r > 0.73$, $p < 0.01$) were also identified between select VOC pairs, such as 1,3-cyclohexadiene (cooked carrot) and α-ionene (earthy); copaene (cooked green) and allo-ocimene (cooked carrot); and α-ionene

(earthy) and nerol oxide (roasted chestnut). Overall, these correlation patterns suggest that co-occurring VOCs may arise from shared biochemical pathways while still contributing uniquely to flavor perception, likely due to differences in odor thresholds, receptor binding, and mixture interactions.

3.3 QTL analysis revealed multiple overlapping hotspots

The 176 differentiating VOCs in the DC population were subjected to QTL analysis. A total of 86 QTLs ($p < 0.00001$) were detected for 61 VOCs in 10 linkage groups (LG2, LG3, LG5, LG6, LG9, LG10, LG11, LG12, LG13, LG14) (Fig. S3). Among the QTLs, 31 were detected for sesquiterpenes, 14 were for monoterpenes, 5 for carotenoid-derived VOCs (apocarotenoids), while only 2 were detected for VOCs derived from SD of amino acids and 4 for VOCs derived from lipid degradation. Twenty QTLs were associated with compounds whose precursors are currently unknown (uncharacterized), and 10 QTLs were associated with compounds that have not been previously reported in mass spectral databases (unknowns) (Table S3). Each QTL explained between 8–39% of the total phenotypic variance. On LG 3, QTLs for two apocarotenoids (α-ionene and α-cyclocitral), 2 monoterpenes (β-terpineol and (+)- Z, E-nepetalactone) and three uncharacterized compounds (2-amino-4-acetamino anisole, 3-methoxy-2,5,6-trimethyl- phenol and 3,4-dimethylbenzyl alcohol) exhibited the highest percentage phenotypic variation (PVE ≥ 30%).

Table 1
Summary statistics of QTLs for VOCs in the DC mapping population. LOP represent the logarithm of p-value score for every genomic position significantly associated with each trait. PVE represent the percentage phenotypic variation explained by each QTL.

Volatile Organic Compound	QTL No	LG No	Position (cM)	Support Interval (cM)	Marker ID	LOP	PVE (%)
Sesquiterpenes							
isocaryophyllene	1	2	155.64	109.42-161.31	S2_4439568	5.38	12
	2	5	127.09	83.13-132.07	S5_22057183	5.54	18
	3	6	32	16.42–41.38	S6_1411677	3.94	9
α-selinene	1	2	155.64	95.17-160.13	S2_4439568	4.16	11
	2	5	106.11	77.45-132.07	S5_20380562	5.07	18
β-selinene	1	2	155.64	101.1-182.01	S2_4439568	4.45	11
	2	5	126.17	71.16–143	S5_21957309	4.52	16
2-carene	1	3	8.11	3.09–30.02	S3_764435	7.67	29
carvacrol	2	3	34.07	3.09–42.31	S3_3318347	6.21	24
humulene	2	5	46.02	42.6-108.12	S5_4598092	5.49	16
α-gurjunene	1	5	56.03	40.34–93.01	S5_6288852	5.31	16
β-cadinene	1	5	85.1	47.02-132.07	S5_18850060	4.12	12
	2	6	30.89	22.74–34.01	S6_4245030	5.83	11
	3	14	118.06	115.08-124.35	S14_16553624	5.63	11
β-panasinsene	1	5	126.17	78.48–143	S5_21957309	4.04	18
γ-dehydro-ar-himachalene	1	5	87.13	44.3-132.07	S5_19044826	4.55	14

Volatile Organic Compound	QTL No	LG No	Position (cM)	Support Interval (cM)	Marker ID	LOP	PVE (%)
Sesquiterpenes							
dehydro-ar-ionene	1	5	87.13	45.26-132.07	S5_19044826	4.76	14
γ-elemene	1	5	72.41	42.6-87.13	S5_16273303	6.21	18
aciphyllene	1	5	56.03	41.24–89.26	S5_6288852	5.82	17
guaiazulene	1	5	87.13	42.6-108.12	S5_19044826	5.71	15
cadina-1(10),6,8-triene	1	5	56.03	42.6-130.13	S5_6288852	4.75	13
cis-calamenene	1	5	87.13	48.43-129.13	S5_19044826	4.93	17
rotundene	1	5	105.43	78.48–147.6	S5_20286795	4.25	16
6,9-guaiadene	1	5	70.33	40.34–87.13	S5_15007205	5.70	17
aristolediene	1	5	101.21	68.26-151.03	S5_19891114	4.39	16
copaene	1	6	30.89	22.74–37.03	S6_4245030	5.62	11
	2	13	96.14	87.33-101.23	S13_18305474	5.88	16
(-)-germacrene D	1	6	30.89	28.16–33.01	S6_4245030	15.65	27
cyclosativene	1	6	32	31.9-34.01	S6_1411677	15.65	31
espatulenol	1	6	33.01	27.65–41.38	S6_12584417	3.97	11
α-cubebene	1	13	97.03	90.22-102.68	S13_18501410	6.01	17
β-cubebene	1	13	97.03	90.22-102.68	S13_18501410	6.01	17
Monoterpenes							
β-terpineol	1	3	26.25	8.11–34.07	S3_2516973	9.15	33

Volatile Organic Compound	QTL No	LG No	Position (cM)	Support Interval (cM)	Marker ID	LOP	PVE (%)
Sesquiterpenes							
	2	12	168	167.02-170.12	S12_22117539	5.84	13
(+)-Z,E,-nepetalactone	1	3	9.05	8.11–31.12	S3_829608	9.23	31
	2	12	168	168-180.09	S12_22117539	5.38	12
camphene	1	3	16.26	8.11–40.44	S3_1308600	7.46	25
	2	12	168	167.02-181.09	S12_22117539	7.81	16
p-thymol	1	3	26.25	7.11–35.02	S3_2516973	8.02	29
	2	12	168	168-170.12	S12_22117539	6.66	16
geraniol	1	9	58.01	33.29–68.1	S9_3113917	5.08	17

Table 1 **(continued)**: Summary statistics of QTLs for VOCs in the DC mapping population. LOP represent the logarithm of p-value score for every genomic position significantly associated with each trait. PVE represent the percentage phenotypic variation explained by each QTL.

Volatile Organic Compound	QTL	LG	Position (cM)	Support Interval (cM)	Marker	LOP	PVE (%)
linalool	1	9	58.01	0.59–58.01	S9_3113917	6.69	21
(E)-linalool oxide	1	9	58.01	30.24–78.01	S9_3113917	6.82	21
(Z)-linalool oxide	1	9	58.01	30.24–78.01	S9_3113917	6.67	21
allo-ocimene	1	9	44.1	0 59-78.01	S9_2217660	4.38	16
(E)-rose oxide	1	10	148.51	146.06-178.55	S10_23066140	4.70	14
Apocarotenoids							
β-ionone	1	3	8.11	3.09–33.02	S3_764435	6.71	24
	2	12	91.12	60.06–168	S12_6681650	3.95	09
α-cyclocitral	1	3	12.11	8.11–29.15	S3_994093	15.65	35
	2	12	168	168-184.15	S12_22117539	6.80	14
α-ionene	1	3	8.11	7.11–28.27	S3_764435	15.65	39
Strecker Degradation							

Volatile Organic Compound	QTL No	LG No	Position (cM)	Support Interval (cM)	Marker ID	LOP	PVE (%)
Sesquiterpenes							
phenylacetaldehyde	1	2	80.08	7.11–28.27	S2_10801073	3.98	39
Fatty acid oxidation							
6-methyl-2-heptanol	1	3	26.25	165.63-176.82	S3_2516973	9.80	13
	2	12	168	10.02–34.07	S12_22117539	5.86	29
3,4-dimethyl-1-pentanol	1	11	83.61	59.22-151.16	S11_5444504	4.00	15
3-ethyl-4-methylpentan-1-ol	1	11	83.61	61.71-157.15	S11_5444504	9.94	15
Unknowns							
phenol, 3-methoxy-2,5,6-trimethyl-	1	3	27.87	8.11–34.07	S3_2575469	15.65	39
	2	12	168	80.16-170.12	S12_22117539	6.19	12
3,4-dimethylbenzyl alcohol	1	3	27.87	8.11–34.07	S3_2575469	15.65	38
	2	12	168	89.01-172.04	S12_22117539	5.35	11
3,3-dimethylcyclohexanone	1	3	12.11	6.02–34.07	S3_994093	15.65	38
	2	12	168	168-180.09	S12_22117539	8.33	15
3,6,6-trimethyl-cyclohex-2-enone	1	3	14	5.06–34.07	S3_1179682	10.06	33
	2	12	168	168-176.82	S12_22117539	7.34	16
1,3-cyclohexadiene	1	3	30.02	3.09–40.44	S3_2945631	4.57	23
2,3,4,5-tetramethyl-2-cyclopenten-1-one	1	3	12.11	7.11–34.07	S3_994093	15.65	38
	2	12	168	168-181.09	S12_22117539	6.61	12
2,3,4,5-tetramethylcyclopent-2-en-1-ol	1	3	8.11	0 32-39.22	S3_764435	15.65	39
	2	12	168	168-184.15	S12_22117539	6.95	13
1-(4-methoxyphenyl)- 1-pentanone	1	3	9.05	5.06–40.44	S3_829608	6.87	29

Volatile Organic Compound	QTL No	LG No	Position (cM)	Support Interval (cM)	Marker ID	LOP	PVE (%)
Sesquiterpenes							
2-amino-4-acetamino anisole	1	3	26.25	7.11–35.02	S3_2516973	15.65	40
	2	12	168	168-170.12	S12_22117539	7.23	14
2-methyl-4-(2,6,6-trimethyl-1-cyclohexenyl)- but-3-enal	1	3	9.05	0-33.02	S3_829608	8.71	32
10-methylundec-3-en-4-olide	1	3	6.02	0-28.27	S3_546844	7.53	28
1,1'-(1,1,10,10-tetramethyl-1,10-decanediyl) bis[3,4-dimethyl-cyclohexanone, 2,2,6-trimethyl-benzene	1	3	14	4.07–34.07	S3_1179682	7.15	31
	1	5	105.43	77.45-129.13	S5_20286795	4.85	17
peak 194	1	3	8.11	4.07–17.11	S3_764435	6.34	19
	2	12	168	67.08-203.49	S12_22117539	4.39	12
peak 479	1	3	8.11	1.27–34.07	S3_764435	6.19	23
peak 787	1	3	14	4.07–34.07	S3_1179682	8.56	32
	2	12	168	150.23-186.21	S12_22117539	4.51	11
peak 2316	1	3	26.25	4.07–35.02	S3_2516973	9.16	31
	2	12	168	91.12-170.12	S12_22117539	5.06	12
peak 504	1	5	106.11	42.6-129.13	S5_20380562	5.33	16
peak 958	1	5	72.41	42.6-107.18	S5_16273303	4.31	13

Table 1 summarizes all identified QTLs in this study, among which 8 QTLs corresponded to 7 of the 27 flavor- associated VOCs. These include two QTLs on LG 6 and 13 for copaene associated with cooked green flavor, one QTL each on LG 9 for geraniol, linalool, (E)- linalool oxide, allo-ocimene, all associated with cooked carrot flavor, one QTL on LG 10 for (E)- rose oxide linked to roasted chestnut flavor, and one QTL on LG 3 for α-ionone associated with earthy flavor. No QTLs were identified for compounds derived from the Maillard reaction (e.g 2- furanmethanol), which have been previously associated with sweetpotato and caramel flavors. Unlike other QTL studies that focused only on flavor-associated compounds, the current study employs a global approach by evaluating all differentiating VOCs based on

their potential precursors, enabling a more comprehensive identification of genetic loci influencing volatile compound profiles.

Several hotspots for overlapping QTLs were detected for VOCs sharing similar precursors, indicating the possibility of highly linked genes or a shared biosynthetic pathway. For example, 17 overlapping QTLs for sesquiterpenes were detected on LG 5 (Fig. 3), seven overlapping QTLs for the monoterpenes were detected on LG 9 (Fig. 4) while three overlapping QTLs were detected for the apocarotenoids on LG 3 (Fig. 5). Hotspots for 12 and 7 overlapping QTLs were also detected for the uncharacterized and unknown compounds on LGs 3 and LG 12 respectively (Fig S4- S5).

The overlapping QTLs spanned large support intervals in similar genomic regions for different traits, showing a possibility of genes for shared pathways. For example, the support interval for the QTLs detected for the apocarotenoids (β-ionone, α-cyclocitral, and α-ionene) on LGs 3, ranged from 3.09–33.03cM (markers S3_764435 – S3_3261239 bp) (Table 1). Similarly, four monoterpenes (β-terpineol, (+)-Z,E-nepetalactone, camphene, p-thymol) overlapped within the same region as the apocarotenoid (Table 1), again indicating the possibility of linked genes or a shared biosynthetic pathway. The support interval of the overlapping QTLs for five monoterpenes (representing geraniol, linalool, (E)-linalool oxide and (Z)-linalool oxide, and allo-ocimene) on LG 9 ranged between 0- 78.01cM (marker S9_59546 – S9_4038847 bp) (Table 1). On linkage groups 3 and 9, ‘Covington’ contributed major alleles (‘b’ for LG 3 and ‘d’ for LG 9) for increasing the means of the apocarotenoids and the monoterpenes (Fig. 6a-d). The presence of a single major positive allele from ‘Covington’ provides evidence that this genotype confers a positive effect to the apocarotenoids and monoterpenes, and this effect could be governed by a single or different colocalized genes on LG 3 and LG 9.

In contrast, QTLs identified on LG 12 for the apocarotenoids and monoterpenes, showed a narrower support interval compared to those on LG 3 and 9 (Table 1), with the parents showing additive allelic effects. Except for the QTLs for β-ionone and (E)-rose oxide, the support interval for other apocarotenoids and monoterpenes on LG 12 were between 167.02–184.15 cM (marker S12_22117539 – S12_23076980). NCDM04-001 contributed a major positive allele ‘i’ to the population means of the apocarotenoids on LG 12 (Fig. 6e-f). Covington also contributed some positive alleles to the apocarotenoids on this linkage group; however, the effect was slightly lower than that of NCDM04-001. This shows the additive effect of these alleles, suggesting that a combination of alleles on LG12 from both parents could be useful for breeding for these traits.

4.0 Discussion

4.1 Sweetpotato VOC Composition and Clustering of QTLs

A total of 176 VOCs differentiated the genotypes in the ‘DC’ mapping population, with sesquiterpenes identified as the most abundant group. This finding is consistent with previous studies that characterized VOCs in the same mapping population (Abugu et al., 2025b) and in sweetpotatoes of varying flesh colors

using GC × GC-ToFMS (Shen et al., 2024). In contrast, other studies using one-dimensional GC-MS reported that compounds from Strecker degradation (SD) of amino acids (such as benzeneacetaldehyde and benzaldehydes) were the most abundant in orange, yellow, and cream-fleshed roots (Yao et al., 2023; Zhang et al., 2023; Zhang et al., 2021). This discrepancy likely reflects differences in the sensitivity and efficiency of the instruments used for VOC analysis and the different methods of sampling. The GC × GC-ToFMS employed in this study is known to be more effective at detecting trace compounds and resolving coeluting compounds, particularly sesquiterpenes, compared to GC-MS (Dimandja, 2003).

The phenotypic distributions of the VOCs in this study revealed substantial variation within the mapping population, highlighting the potential diversity of flavor-related traits available for genetic analysis. As observed in approximately 13% of the VOCs, some progeny exhibited phenotypic values beyond those of both parental lines, indicating a likelihood of transgressive segregation for those traits in the DC population. Distribution shapes also ranged from near-symmetrical to skewed, bimodal, or irregular patterns, reflecting non-uniform segregation of volatile abundance across the population. A similar non-uniform segregation pattern have been previously reported in other crops. For example, Yang et al. 2023, reported transgressive segregation in 10 VOCs with a wide range of variation for VOCs identified in progenies in an apple fruit mapping population. Similarly, Christeller et al., 2019 reported that out of the 77 total VOCs identified in apple peels, nine, 41 and 27 of them displayed bimodal, skewed and normal distributions, respectively. Other studies using mapping populations in grape hybrid (Koyama et al., 2022) and tomatoes (Tieman et al., 2006) further illustrate distribution patterns that depart from simple normality for flavor-associated VOCs. This heterogeneity across compounds underscores the complexity of VOC phenotypes while confirming that sufficient variation exists for effective QTL mapping. Overall, these findings provide a strong phenotypic basis for mapping genomic regions linked to volatile composition and offer valuable insight for molecular breeding strategies focused on enhancing flavor quality.

The correlation-based clustering of VOCs, together with co-localization of QTLs further indicated that certain VOCs may be influenced by shared genomic regions. In our study, correlation-based clustering grouped 39 sesquiterpene VOCs together. Across these VOCs, 31 QTLS were identified, 16 of which co-localized within the same genomic region. This pattern suggests that a few genomic regions may jointly regulate the abundance of many sesquiterpene VOCs within this chemical class. Similar clustering patterns of sesquiterpenes and their QTLs have been reported in other crops. For example, Yu et al., (2017) found that 18 out of 27 sesquiterpenes in citrus clustered together, and 41 corresponding QTLs also localized to four genomic regions. Other studies in apples (Dunemann et al, 2009), tomato (Zanor et al., 2009), almonds (Sanchez-Perez et al., 2007) and peach (Eduardo et al., 2013) revealed a similar pattern. Genes involved in terpene synthesis are often organized in clusters through tandem duplication, as previously reported in multiple plant genomes (Jiang et al., 2019), which may explain why several monoterpene VOCs mapped to the same genomic regions. In our study, strong phenotypic correlations were observed among some monoterpenes, with five out of ten monoterpenes mapping to chromosome 9, reflecting coordinated accumulation and a potential hotspot for monoterpene regulation.

Interestingly, the subset of monoterpenes previously identified as top flavor predictors did not consistently exhibit strong correlations or overlapping QTLs. For example, (E)-rose oxide and nerol oxide were strongly correlated (r = 0.80), yet only a single QTL was detected for (E)-rose oxide. Conversely, geraniol and linalool (both associated with cooked carrot flavor), which showed a weak correlation (r = 0.39), mapped to overlapping QTL regions. These patterns likely reflect the complex biosynthetic pathways of monoterpenes, including enzyme specificity, pathway branching, and, as well as contributions from minor-effect loci or environmental variation. Although both geraniol and linalool are derived from a common precursor, their production is controlled by distinct enzymes and may be differentially regulated across genotypes or developmental stages, explaining the weak correlation observed between them (Iijima et al., 2004).

The weak correlation patterns and lack of QTL co-localization for compounds derived from MR and sugar caramelization (e.g., 2-furanmethanol, acetone, pyrrole, furan), SD of amino acids (e.g., phenylacetaldehyde, methional, benzaldehyde, benzenethanol), and fatty acid oxidation (e.g. hexanal, nonanal, 1-pentanol) suggests that their substrates vary across the population, and their formation is influenced by multiple interacting factors and complex biochemical processes. For example, the MR-derived VOCs are formed through multifaceted chemical reactions between reducing sugars and amino acids (Kays & Wang, 2000; Sun et al., 1995). In a complex food matrix, reactive carbonyl compounds produced during the MR, SD and fatty acid oxidation could participate in cross reactions to generate novel VOCs (Farmer & Mottram, 1990; Mastrocola et al., 2000; Troise et al., 2020). Because the formation of one VOC can divert shared precursors into alternative products, the levels of different VOCs do not necessarily rise or fall together. This cross-reaction likely explains the weak correlation patterns observed for these VOCs. In addition, the absence of QTLs for most MR-derived compounds is not surprising, as their formation is driven primarily by chemical reactions rather than enzymatic reactions that are under direct genetic control (Kays & Wang, 2000; Sun et al., 1995).

4.2 Genetic Architecture of Flavor-Associated VOCs in Sweetpotato

To the best of our knowledge, information on the genetic control of flavor-associated VOCs in sweetpotato has not been previously reported, and the present study provides the first foundation for elucidating the genetic mechanism controlling VOCs in this crop. In an earlier study, 27 compounds that contributed to the prediction of 10 flavor traits in cooked sweetpotato were reported (Abugu et al., 2025b). However, in the current study, few QTLs were identified for the VOCs associated with these flavor attributes. For example, no QTLs were detected for the top VOCs known to positively impact “caramel” flavor (e.g., 2- furanmethanol). As discussed above, these top predictors were VOCs potentially generated during MR, which is a complex non-enzymatic chemical process. This fact may explain the lack of QTLs detected for these VOCs in this study.

In contrast, two QTLs were detected for geraniol and linalool, monoterpenes associated with ‘cooked carrot’ flavor in sweetpotato. Our previous study also highlighted the contribution of two apocarotenoids,

β-ionone and α-cyclocitral, to cooked carrot flavor, although at moderate levels (Abugu et al., 2025b, Table S7). In this study, four QTLs were identified for the apocarotenoids on two linkage groups. QTLs for monoterpenes, including linalool and geraniol, have been reported in other crops such as carrots (Keilwagen et al., 2017), grapes (Koyama et al., 2022), and tea tree (Voelker et al., 2023), while QTLs for apocarotenoids, including β-ionone and α-cyclocitral, were found in tomato (Mathieu et al., 2009; Smikin et al., 2004). Together, these cross-species parallels suggest a conserved genetic architecture underlying volatile compound biosynthesis and support the biological relevance of the QTLs identified in sweetpotato.

The apocarotenoid QTLs identified in this study, span the same genetic and genomic regions with the QTLs previously reported for β-carotene (the main precursors of apocarotenoids) in the DC (Kinczyk 2019) and a Beauregard x Tanzania (BT) mapping population (Gemenet et al., 2020). Both studies identified two major β-carotene QTLs on LGs 3 and 12. Kinczyk (2019) reported ranges of 30.02–33.02cM on LG 3 and 168.00–170cM on LG 12; whereas Gemenet et al., (2020) reported broader ranges 0.00–121cM on LG 3 and 124.12–176.02cM on LG 12 (Table S4). The β-ionone QTL identified in our study (3.00–33.02 cM on LG 3 and 60.06–168 on LG 12) colocalized with the previously reported β-carotene QTLs, supporting the validity of our findings. Importantly, the monoterpene QTLs reported here represent the first of such findings in sweetpotato, underscoring the novelty and potential impact of this study for future flavor-focused breeding efforts.

The ‘Covington’ alleles exerted the biggest positive effect for most apocarotenoids and monoterpene QTLs on LG 3 and 9 (Fig. 6). In contrast, on LG 12, “NCDM04-001” carried an allele (i) responsible for a positive allelic effect on apocarotenoids, with smaller positive allelic contributions from ‘Covington’. As previously reported for BC (Kinczyk, 2019), the allelic effects for the VOCs were additive. Thus, individuals inheriting alleles ‘c’ and ‘d’ from ‘Covington’ on LG 3, and allele ‘i’ from NCDM04-001 for LG12 QTLs, would be expected to accumulate higher levels of apocarotenoids. While individuals inheriting allele “b” from Covington on LG 9 would be expected to have high levels of the monoterpenes associated with cooked carrot flavor. Prior consumer research in African populations suggest that a high ‘cooked carrot’ flavor may not be a desirable trait in sweetpotato (Laurie et al., 2013), although this has not yet been evaluated among US consumers. Therefore, if this flavor is ultimately found undesirable in the US market, the positive alleles ‘b’ and ‘d’ from ‘Covington’ on LG 3; alleles “b’ from Covington on LG 9 and the additive alleles ‘i’ and ‘c’ from NCDM04-001 and ‘Covington’ respectively on LG 12 would likely need to be selected against to reduce the ‘cooked carrot’ flavor perception in sweetpotato. However, a consumer acceptance study in the U.S is needed to determine whether this flavor attribute impacts sweetpotato liking before these alleles should be targeted for selection in breeding programs.

4.3 Shared Genetic Control of Carotenoid and Apocarotenoid VOCs

Our QTL analysis also revealed regions with shared genetic control or pleiotropic interactions. Several genes involved in BC accumulation, degradation and the formation of apocarotenoids (including the

geranylgeranyl pyrophosphate synthase (GGPP), phytoene synthase (PSY), carotenoid cleavage dioxygenases (CCDs) and 9-cis-epoxycarotenoid cleavage dioxygenases (NCEDs) have been well characterized in sweetpotato (Park et al., 2020; Zhang et al., 2023). CCDs and NCEDs catalyze the conversion of BC into apocarotenoids (such as β-ionone and α-cyclocitral). While in depth candidate gene characterization was not performed in this study, we observed a NAC domain- containing protein overlapping with the QTL peak (S3_764435) identified for β-ionone on LG 3. This genomic region contains 130 genes in diploid sweetpotato (Yan et al., 2021) and is also represented in a haplotype-resolved chromosome level hexaploid sweetpotato genome assembly (Wu et al., 2025). Among these genes, IbNAC29 has been shown to positively regulate BC accumulation in sweetpotato, through forming a regulatory module that up-regulates carotenoid biosynthesis gene IbPSY (Xing et al., 2023). Interestingly, the GGPP (itf03g04380) and PSY (itf03g05110) co-localized within the confidence interval (S3_221,008 and S3_3,261,239) of the apocarotenoid QTLs on LG 3. The presence of genes involved in carotenoid biosynthesis within the confidence interval of the apocarotenoids supports the possibility of shared genetic control or pleiotropic interactions, consistent with previous observations in sweetpotato (Park et al., 2020; Zhang et al., 2023).

The colocalization of apocarotenoid QTLs with previously identified QTLs for BC provides a potential road map for molecular marker identification. For example, the α-cyclocitral QTL peak (S12_22117539) overlaps with that of BC QTLs reported by Kinczyk (2019) and Gemenet et al., (2020), which is expected given that cyclocitrals are a direct degradation product of BC (Ramel et al., 2012). Previous studies also reported the presence of an IbOr gene (itf12g24270) located between 22,122,009 kb and 22,124,719 kb with the BC support interval of 125.25-205.67 cM (Gemenet et al., 2020, Kinczyk 2019). This positions the α-cyclocitral QTL on LG 12 (marker S12_22117539) within ~ 4.5 kb of this IbOr, suggesting that the genes controlling both BC accumulation and its degradation may be genetically linked or possibly pleiotropic. Similar observations have been reported in other crops, where carotenoid loci influence the emission of carotenoid-derived volatiles in tomato (Mathieu et al., 2009; Simkin et al., 2004; Tieman et al., 2006), apricot (Xi et al., 2020), and peach (Brandi et al., 2011). While our results indicate that a single marker (S12_22117539) could be leveraged to select for both metabolites on LG 12, a separate marker would be required to specifically select for the α-cyclocitral QTL on LG 3 if the trait is desired in breeding programs.

4.4 Shared Genetic Control of Monoterpene VOCs and Terpene Synthase Gene Clusters

For the monoterpenes, a functional annotation search revealed ten terpene synthase genes colocalized with the QTLs for geraniol and linalool. These genes (Table S5) are located between 2,839,581–2,918,485 bp and fall within the support interval of 0–58.01cM (59546- 3567478) for both geraniol and linalool on LG 9. The terpene synthase gene clusters, reported as linalool synthase, (3S)-linalool/(E)-nerolidol /(E,E)-geranyl linalool synthase have been characterized in other crops (Lavy, 2002; Van Schie et al., 2007; Zhou et al., 2020), and are directly involved in the production of linalool and geraniol. The presence of these multiple genes involved in both monoterpenes is consistent as previous studies have

shown that terpene synthases can undergo transcript splicing, generating functional diversity and contributing to the formation of multiple compounds from the same genomic region, as reported in tea plants (Liu et al., 2018). Together, these observations highlight candidate genes underlying monoterpene variation and suggest shared genetic control, providing potential targets for marker-assisted selection in sweetpotato breeding programs.

4.5 Limitations of Current Study and Pathways for Further Research

The limitations of this study include that the storage roots used for analysis were baked under simulated conditions in headspace vials, and the core sampling method used does not account for potential within-root variability. In addition, all of the materials, i.e. progenies, used in these studies were only evaluated from a single location during one growing season. Since VOC profiles are thought to be influenced by environmental factors, the stability of the QTLs identified here may be affected by genotype × environment (G×E) interactions. Nevertheless, QTLs detected at the same genomic positions for multiple related compounds suggest that these loci may be stable and reliable; though, the candidate genes within these intervals remain putative. Future work will focus on validating these QTLs across multiple locations, years, and in different populations to determine the stability of the QTLs, and on refining candidate gene identification through fine mapping and comparative transcriptome analysis.

5.0 Conclusions

This study provides insight into the genetic architecture of VOCs in sweetpotato. Volatile compound profiles were evaluated using GC × GC-ToFMS in an “NCDM04_001” x “Covington” mapping population, and the genetics underlying the phenotypic variation in VOCs were dissected. A total of 86 QTLs were detected for 61 volatile compounds across 10 linkage groups. Groups of VOCs and QTLs from similar biochemical pathways often mapped into overlapping regions. Based on their potential precursors, several hotspots for overlapping QTLs were identified, suggesting the presence of highly linked genes and/or shared biosynthetic pathways. While many of the major VOCs that drive the characteristic sweetpotato flavor may be under chemical or complex genetic control, the monoterpenes and apocarotenoids associated with ‘cooked carrot’ flavor may be controlled by different tightly linked genes or a single gene with pleiotropic effects. The effect of the alleles at some of the QTLs were additive as the overall genetic impact of VOCs was distributed across numerous genetically and functionally independent loci. To the best of our knowledge, the QTLs described in this study are the first to be reported for VOCs in cooked sweetpotato. The QTLs for key flavor-associated compounds identified in this study will facilitate the development of molecular markers for screening flavor traits at the genetic level and enable breeders to more precisely incorporate consumer-preferred flavors into new varieties. Additionally, this study provides a framework for future investigations of VOCs linked to sweetpotato flavors that may not be under strong genetic control, including the potential effects of environmental influences on sweetpotato flavor traits.

Declarations

Competing Interests

The authors have no relevant financial or non-financial interests to disclose.

Funding

This study was funded by royalty receipts from the Sweetpotato and Potato Breeding and Genetics Program, North Carolina State University (NCSU), Raleigh, NC, and funding from the Bill and Melinda Gates Foundation via a subcontract with the International Potato Center, Lima, Peru under the RTB Breeding Project (CGIAR Investment ID1523-BMGF). Instrumentation and technical support were provided by the USDA-ARS Food Science and Market Quality & Handling Research Unit, Raleigh, NC. M.I. and M.A. were also supported by the United States Department of Agriculture National Institute of Food and Agriculture, Hatch project 1008691. MA was also partially funded through NC State University Genetics & Genomics Scholars Fellowship and the NSF-NRT Graduate Training Grant 1828820. M.M. was partially supported by the Agriculture and Food Research Initiative, project award no. 2022-67013-36269, from the U.S. Department of Agriculture's National Institute of Food and Agriculture. Any opinions, findings, conclusions, or recommendations expressed in this publication are those of the authors and should not be construed to represent any official USDA or U.S. Government determination or policy.

Author Contribution

Modesta Abugu: Conceptualization; Investigation; methodology; validation; visualization; writing—original draft; writing—review and editing; formal analysis. **Gabriel De Siqueira Gesteira:** Methodology, formal analysis; validation; visualization; writing—review and editing. **Suzanne D. Johanningsmeier** : Conceptualization; investigation; resources; supervision; writing—review and editing. **Marcelo Mollinari:** Methodology; writing—review and editing. **Bode Olukolu:** Methodology; writing—review and editing. **Ken Pecota:** Conceptualization, methodology, resources; **Massimo Iorizzo:** Conceptualization; writing—review and editing; methodology, supervision, resources; project administration. **G. Craig Yencho:** Conceptualization; writing—review and editing; methodology supervision; resources; project administration.

Acknowledgement

We greatly appreciate the project team members of Yencho lab and the Horticultural Crops Research Station (HCRS) for their assistance with planting and harvesting of the DC population. We also thank members of the the Johanningsmeier's lab, and Emily Genther of the Sweetpotato Breeding and Genetics Program for administrative and programming support.

Data Availability

The datasets generated during and analyzed from this study are available from the corresponding author on reasonable request.

References

1. Abugu, M., Allan, M., Johanningsmeier, S., Iorizzo, M., & Yencho, G. C. (2025a). Comprehensive review of sweetpotato flavor compounds: Opportunities for developing consumer-preferred varieties. *Comprehensive Reviews in Food Science and Food Safety*, *24*(3), e70172. https://doi.org/10.1111/1541-4337.70172
2. Abugu, M. N. (2025b). Volatile composition, sensory attributes and Quantitative Trait Loci (QTLs) associated with flavor traits in cooked Sweetpotato. [Dissertation]. [Raleigh (NC)]: North Carolina State University. http://dx.doi.org/10.2139/ssrn.5436894
3. Bassett, A., Katuuramu, D. N., Song, Q., & Cichy, K. (2021). QTL mapping of seed quality traits including cooking time, flavor, and texture in a yellow dry bean (Phaseolus vulgaris L.) Population. *Frontiers in Plant Science*, *12*, 670284. https://doi.org/10.3389/fpls.2021.670284
4. Brandi, F., Bar, E., Mourgues, F., Horváth, G., Turcsi, E., Giuliano, G., Liverani, A., Tartarini, S., Lewinsohn, E., & Rosati, C. (2011). Study of “Redhaven” peach and its white-fleshed mutant suggests a key role of CCD4 carotenoid dioxygenase in carotenoid and norisoprenoid volatile metabolism. BMC Plant Biology, 11(1), 24. https://doi.org/10.1186/1471-2229-11-24
5. Cervantes-Flores, J. C., Sosinski, B., Pecota, K. V., Mwanga, R. O. M., Catignani, G. L., Truong, V. D., Watkins, R. H., Ulmer, M. R., & Yencho, G. C. (2011). Identification of quantitative trait loci for dry-matter, starch, and β-carotene content in sweetpotato. *Molecular Breeding*, *28*(2), 201–216. https://doi.org/10.1007/s11032-010-9474-5
6. Christeller, J. T., McGhie, T. K., Johnston, J. W., Carr, B., & Chagné, D. (2019). Quantitative trait loci influencing pentacyclic triterpene composition in apple fruit peel. *Scientific Reports*, *9*(1), 18501. https://doi.org/10.1038/s41598-019-55070-5
7. Chen, Y., Liu, Y., & Feng, X. (2023). Food Perception: Taste, Smell and Flavour. Foods, 12(19), 3628. https://doi.org/10.3390/foods12193628
8. Costa, F., Cappellin, L., Zini, E., Patocchi, A., Kellerhals, M., Komjanc, M., Gessler, C., & Biasioli, F. (2013). QTL validation and stability for volatile organic compounds (VOCs) in apple. Plant Science, 211, 1–7. https://doi.org/10.1016/j.plantsci.2013.05.018
9. Da Silva Pereira, G., Gemenet, D. C., Mollinari, M., Olukolu, B. A., Wood, J. C., Diaz, F., Mosquera, V., Gruneberg, W. J., Khan, A., Buell, C. R., Yencho, G. C., & Zeng, Z.-B. (2020). Multiple QTL Mapping in Autopolyploids: A random-effect model approach with application in a hexaploid Sweetpotato full-sib population. Genetics, 215(3), 579–595. https://doi.org/10.1534/genetics.120.303080
10. Dunemann, F., Ulrich, D., Boudichevskaia, A., Grafe, C., & Weber, W. E. (2009). QTL mapping of aroma compounds analysed by headspace solid-phase microextraction gas chromatography in the apple

progeny ‘Discovery’×‘Prima’. *Molecular breeding*, *23*, 501–521. https://doi.org/10.1007/s11032-008-9252-9

11. Dimandja, J. M. D. (2003). A new tool for the optimized analysis of complex volatile mixtures: Comprehensive two-dimensional gas chromatography/lime-of-flight mass spectrometry. *American laboratory (Fairfield)*, *35*(3), 42–53. http://pascal-francis.inist.fr/vibad/index.php?action=getRecordDetail&idt=14571186
12. Eduardo, I., Chietera, G., Pirona, R., Pacheco, I., Troggio, M., Banchi, E., & Pozzi, C. (2013). Genetic dissection of aroma volatile compounds from the essential oil of peach fruit: QTL analysis and identification of candidate genes using dense SNP maps. *Tree genetics & genomes*, *9*(1), 189–204. https://doi.org/10.1007/s11295-012-0546-z
13. Farmer, L. J., & Mottram, D. S. (1990). Interaction of lipid in the maillard reaction between cysteine and ribose: The effect of a triglyceride and three phospholipids on the volatile products. Journal of the Science of Food and Agriculture, 53(4), 505–525. https://doi.org/10.1002/jsfa.2740530409
14. Fraher, S., Schwarz, T., Heim, C., De Siqueira Gesteira, G., Mollinari, M., Da Silva Pereira, G., Zeng, Z.-B., Brown-Guedira, G., Gorny, A., & Yencho, G. C. (2024). Discovery of a major QTL for resistance to the guava root-knot nematode (Meloidogyne enterolobii) in ‘Tanzania’, an African landrace sweetpotato (Ipomoea batatas). *Theoretical and Applied Genetics*, *137*(10), 234. https://doi.org/10.1007/s00122-024-04739-1
15. Gemenet, D. C., Da Silva Pereira, G., De Boeck, B., Wood, J. C., Mollinari, M., Olukolu, B. A., Diaz, F., Mosquera, V., Ssali, R. T., David, M., Kitavi, M. N., Burgos, G., Felde, T. Z., Ghislain, M., Carey, E., Swanckaert, J., Coin, L. J. M., Fei, Z., Hamilton, J. P., Buell, C. R. (2020). Quantitative trait loci and differential gene expression analyses reveal the genetic basis for negatively associated β-carotene and starch content in hexaploid sweetpotato [Ipomoea batatas (L.) Lam.]. *Theoretical and Applied Genetics*, *133*(1), 23–36. https://doi.org/10.1007/s00122-019-03437-7
16. George, J., Reddy, G. V. P., Wadl, P. A., Rutter, W., Culbreath, J., Lau, P. W., Rashid, T., Allan, M. C., Johaningsmeier, S. D., Nelson, A. M., Wang, M. L., Gubba, A., Ling, K., Meng, Y., Collins, D. J., Ponniah, S. K., & Gowda, P. H. (2024). Sustainable sweetpotato production in the United States: current status, challenges, and opportunities. Agronomy Journal, 116(2), 630–660. https://doi.org/10.1002/agj2.21539
17. Haque, E., Tabuchi, H., Monden, Y., Suematsu, K., Shirasawa, K., Isobe, S., & Tanaka, M. (2020). QTL analysis and GWAS of agronomic traits in sweetpotato (Ipomoea batatas L.) using genome wide SNPs. Breeding Science, 70(3), 283–291. https://doi.org/10.1270/jsbbs.19099
18. Haque, E., Yamamoto, E., Shirasawa, K., Tabuchi, H., Yoon, U.-H., Isobe, S., & Tanaka, M. (2020). Genetic analyses of anthocyanin content using polyploid GWAS followed by QTL detection in the sweetpotato (Ipomoea batatas L.) storage root. Plant Root, 14(0), 11–21. https://doi.org/10.3117/plantroot.14.11
19. Iijima Y, Davidovich-Rikanati R, Fridman E, Gang DR, Bar E, Lewinsohn E, Pichersky E (2004). The biochemical and molecular basis for the divergent patterns in the biosynthesis of terpenes and

phenylpropenes in the peltate glands of three cultivars of basil. Plant Physiol.136(3):3724–36. https://doi.org/10.1104/pp.104.051318

20. Jiang, S. Y., Jin, J., Sarojam, R., & Ramachandran, S. (2019). A comprehensive survey on the terpene synthase gene family provides new insight into its evolutionary patterns. *Genome biology and evolution*, *11*(8), 2078–2098. https://doi.org/10.1093/gbe/evz142
21. Kassambara, A. (2016). ggcorrplot: Visualization of a Correlation Matrix using "ggplot2" (p. 0.1.4.1) [Dataset]. https://doi.org/10.32614/CRAN.package.ggcorrplot
22. Kassambara, A., & Mundt, F. (2016). factoextra: Extract and Visualize the Results of Multivariate Data Analyses (p. 1.0.7). https://doi.org/10.32614/CRAN.package.factoextra
23. Kays, S. J., & Wang, Y. (2000). Thermally Induced Flavor Compounds. HortScience, 35(6), 1002–1012. https://doi.org/10.21273/HORTSCI.35.6.1002
24. Kays, S. J. (2005). Flavor-the key to sweetpotato consumption. In *II International Symposium on Sweetpotato and Cassava: Innovative Technologies for Commercialization 703* (pp. 97–106). https://doi.org/10.17660/ActaHortic.2006.703.10
25. Keilwagen, J., Lehnert, H., Berner, T., Budahn, H., Nothnagel, T., Ulrich, D., & Dunemann, F. (2017). The terpene synthase gene family of Carrot (Daucus carota L.): Identification of QTLs and candidate genes associated with terpenoid volatile compounds. Frontiers in Plant Science, 8, 1930. https://doi.org/10.3389/fpls.2017.01930
26. Kinczyk, J. (2019). Discovery and analysis of QTL for important processing traits and resistance to Fusarium oxysporum f. Sp. Batatas in the NCDM04-0001× Covington Sweetpotato mapping population [North Carolina State University.]. https://proxying.lib.ncsu.edu/index.php/login?url=https://www.proquest.com/dissertations-theses/discovery-analysis-qtl-important-processing/docview/2405488352/se-2
27. Koyama, K., Kono, A., Ban, Y., Bahena-Garrido, S. M., Ohama, T., Iwashita, K., Fukuda, H., & Goto-Yamamoto, N. (2022). Genetic architecture of berry aroma compounds in a QTL (quantitative trait loci) mapping population of interspecific hybrid grapes (Vitis labruscana × Vitis vinifera). *BMC Plant Biology*, *22*(1), 458. https://doi.org/10.1186/s12870-022-03842-z
28. Laurie, S. M., Faber, M., Calitz, F. J., Moelich, E. I., Muller, N., & Labuschagne, M. T. (2013). The use of sensory attributes, sugar content, instrumental data and consumer acceptability in selection of sweet potato varieties. *Journal of the Science of Food and Agriculture*, *93*(7), 1610–1619. https://doi.org/10.1002/jsfa.5932
29. Lavy, M., Zuker, A., Lewinsohn, E., Larkov, O., Ravid, U., Vainstein, A., & Weiss, D. (2002). Linalool and linalool oxide production in transgenic carnation flowers expressing the Clarkia breweri linalool synthase gene. *Molecular Breeding*, *9*, 103–111. https://doi.org/10.1023/A:1026755414773
30. Liu, G., Liu, J., He, Z., Wang, F., Yang, H., Yan, Y., Gao, M., Gruber, M. Y., Wan, X., & Wei, S. (2018). Implementation of CsLIS/NES in linalool biosynthesis involves transcript splicing regulation in Camellia sinensis. Plant, Cell & Environment, 41(1), 176–186. https://doi.org/10.1111/pce.13080

31. Martina, M., Tikunov, Y., Portis, E., & Bovy, A. G. (2021). The genetic basis of tomato aroma. *Genes*, *12*(2), 226. https://doi.org/10.3390/genes12020226
32. Mastrocola, D., Munari, M., Cioroi, M., & Lerici, C. R. (2000). Interaction between Maillard reaction products and lipid oxidation in starch-based model systems. Journal of the Science of Food and Agriculture, 80(6), 684–690. https://doi.org/10.1002/(sici)1097-0010(20000501)
33. Mathieu, S., Cin, V. D., Fei, Z., Li, H., Bliss, P., Taylor, M. G., Klee, H. J., & Tieman, D. M. (2009). Flavour compounds in tomato fruits: Identification of loci and potential pathways affecting volatile composition. Journal of Experimental Botany, 60(1), 325–337. https://doi.org/10.1093/jxb/ern294
34. Mollinari, M., Olukolu, B. A., Pereira, G. D. S., Khan, A., Gemenet, D., Yencho, G. C., & Zeng, Z.-B. (2020). Unraveling the Hexaploid Sweetpotato inheritance using ultra-dense multilocus mapping. G3 Genes|Genomes|Genetics, 10(1), 281–292. https://doi.org/10.1534/g3.119.400620
35. Oloka, B. M., Da Silva Pereira, G., Amankwaah, V. A., Mollinari, M., Pecota, K. V., Yada, B., Olukolu, B. A., Zeng, Z.-B., & Craig Yencho, G. (2021). Discovery of a major QTL for root-knot nematode (Meloidogyne incognita) resistance in cultivated sweetpotato (Ipomoea batatas). Theoretical and Applied Genetics, 134(7), 1945–1955. https://doi.org/10.1007/s00122-021-03797-z
36. Park, S.-C., Kang, L., Park, W. S., Ahn, M.-J., Kwak, S.-S., & Kim, H. S. (2020). Carotenoid cleavage dioxygenase 4 (CCD4) cleaves β-carotene and interacts with IbOr in sweetpotato. Plant Biotechnology Reports, 14(6), 737–742. https://doi.org/10.1007/s11816-020-00649-y
37. Qu L, Guennel T, Marshall SL. 2013. “Linear score tests for variance components in linear mixed models and applications to genetic association studies.” Biometrics 69 (4): 883–892. https://doi.org/10.1111/biom.12095
38. Rickman, T.E., Adams, A.K., Wadl, P.A. (2025). Genome-wide associations of sweetpotato metabolites enhance genomic prediction and identify genes in metabolic and regulatory pathways. Sci Rep 15, 9657 https://doi.org/10.1038/s41598-025-93415-5
39. Ramel, F., Birtic, S., Ginies, C., Soubigou-Taconnat, L., Triantaphylidès, C., & Havaux, M. (2012). Carotenoid oxidation products are stress signals that mediate gene responses to singlet oxygen in plants. *Proceedings of the National Academy of Sciences*, *109*(14), 5535–5540. https://doi.org/10.1073/pnas.1115982109
40. Sánchez-Pérez, R., Howad, W., Dicenta, F., Arús, P., & Martínez-Gómez, P. (2007). Mapping major genes and quantitative trait loci controlling agronomic traits in almond. Plant Breeding, 126(3), 310–318. https://doi.org/10.1111/j.1439-0523.2007.01329.x
41. Shen, X., Wang, H., Yao, L., Song, S., Wang, H., Sun, M., Liu, Q., Yu, C., & Feng, T. (2024). Volatile compounds analysis and sensory profiling of four colored roasted sweet potatoes via HS-SPME GC-O-MS and HS-SPME GC×GC-TOF MS. Journal of Food Composition and Analysis, 131, 106256. https://doi.org/10.1016/j.jfca.2024.106256
42. Simkin, A. J., Schwartz, S. H., Auldridge, M., Taylor, M. G., & Klee, H. J. (2004). The tomato carotenoid cleavage dioxygenase 1 genes contribute to the formation of the flavor volatiles β -ionone,

pseudoionone, and geranylacetone. The Plant Journal, 40(6), 882–892. https://doi.org/10.1111/j.1365-313X.2004.02263.x

43. Sun, J.-B., Severson, R. F., Schlotzhauer, W. S., & Kays, S. J. (1995). Identifying Critical Volatiles in the Flavor of Baked `Jewel' Sweetpotatoes [Ipomoea batatas (L.) Lam.]. Journal of the American Society for Horticultural Science, 120(3), 468–474. https://doi.org/10.21273/jashs.120.3.468
44. Tieman, D. M., Zeigler, M., Schmelz, E. A., Taylor, M. G., Bliss, P., Kirst, M., & Klee, H. J. (2006). Identification of loci affecting flavour volatile emissions in tomato fruits. Journal of Experimental Botany, 57(4), 887–896. https://doi.org/10.1093/jxb/erj074
45. Troise, A. D., Fogliano, V., Vitaglione, P., & Berton-Carabin, C. C. (2020). Interrelated Routes between the Maillard Reaction and Lipid Oxidation in emulsion systems. Journal of Agricultural and Food Chemistry, 68(43), 12107–12115. https://doi.org/10.1021/acs.jafc.0c04738
46. Van Schie, C. C. N., Haring, M. A., & Schuurink, R. C. (2007). Tomato linalool synthase is induced in trichomes by jasmonic acid. Plant Molecular Biology, 64(3), 251–263. https://doi.org/10.1007/s11103-007-9149-8
47. Voelker, J., Mauleon, R., & Shepherd, M. (2023). A terpene synthase supergene locus determines chemotype in Melaleuca alternifolia (tea tree). New Phytologist, 240(5), 1944–1960. https://doi.org/10.1111/nph.19262
48. Wadl, P. A., Olukolu, B. A., Branham, S. E., Jarret, R. L., Yencho, G. C., & Jackson, D. M. (2018). Genetic diversity and population structure of the USDA Sweetpotato (Ipomoea batatas) Germplasm Collections Using GBSpoly. Frontiers in Plant Science, 9, 1166. https://doi.org/10.3389/fpls.2018.01166
49. Wang, Y., Horvat, R. J., White, R. A., & Kays, S. J. (1996). Influence of postharvest curing treatment on the synthesis of the volatile flavor components in sweetpotato. In International Postharvest Science Conference Postharvest 96 464 (pp. 207–212). https://doi.org/10.17660/ActaHortic.1998.464.29
50. Wang, Y., & Kays, S. J. (2001). Effect of cooking method on the aroma constituents of sweet potatoes [Ipomoea batatas]. Journal of Food Quality, 24(1), 67–78. https://doi.org/10.1111/j.1745-4557.2001.tb00591.x
51. Wickham, H., Chang, W., Henry, L., Pedersen, T. L., Takahashi, K., Wilke, C., Woo, K., Yutani, H., Dunnington, D., & Van Den Brand, T. (2007). ggplot2: Create Elegant Data Visualisations Using the Grammar of Graphics (p. 3.5.1) [Dataset]. https://doi.org/10.32614/CRAN.package.ggplot2
52. Wu, S., Lau, K. H., Cao, Q., Hamilton, J. P., Sun, H., Zhou, C., Eserman, L., Gemenet, D. C., Olukolu, B. A., Wang, H., Crisovan, E., Godden, G. T., Jiao, C., Wang, X., Kitavi, M., Manrique-Carpintero, N., Vaillancourt, B., Wiegert-Rininger, K., Yang, X., Fei, Z. (2018). Genome sequences of two diploid wild relatives of cultivated sweetpotato reveal targets for genetic improvement. Nature Communications, 9(1), 4580. https://doi.org/10.1038/s41467-018-06983-8
53. Wu, S., Sun, H., Zhao, X., Hamilton, J. P., Mollinari, M., Gesteira, G. D. S., Fei, Z. (2025). Phased chromosome-level assembly provides insight into the genome architecture of hexaploid sweetpotato. *Nature Plants*, *11*(9), 1951–1959. https://doi.org/10.1038/s41477-025-02079-6

54. Xi, W., Zhang, L., Liu, S., & Zhao, G. (2020). The genes of CYP, ZEP, and CCD1/4 play an important role in controlling carotenoid and aroma volatile apocarotenoid accumulation of apricot fruit. Frontiers in Plant Science, 11, 607715. https://doi.org/10.3389/fpls.2020.607715
55. Xing, S., Li, R., Zhao, H., Zhai, H., He, S., Zhang, H., Zhou, Y., Zhao, N., Gao, S., & Liu, Q. (2023). The transcription factor IbNAC29 positively regulates the carotenoid accumulation in sweet potato. Horticulture Research, 10(3), uhad010. https://doi.org/10.1093/hr/uhad010
56. Yada, B., Brown-Guedira, G., Alajo, A., Ssemakula, G. N., Owusu-Mensah, E., Carey, E. E., Mwanga, R. O. M., & Yencho, G. C. (2017). Genetic analysis and association of simple sequence repeat markers with storage root yield, dry matter, starch and β-carotene content in sweetpotato. Breeding Science, 67(2), 140–150. https://doi.org/10.1270/jsbbs.16089
57. Yan, H., Ma, G., Teixeira da Silva, J. A., Qiu, L., Xu, J., Zhou, H., & Tang, X. (2021). Genome-wide identification and analysis of NAC transcription factor family in two diploid wild relatives of cultivated sweet potato uncovers potential NAC genes related to drought tolerance. Frontiers in Genetics, 12, 744220. https://doi.org/10.3389/fgene.2021.744220
58. Yang, S., Yu, J., Yang, H., & Zhao, Z. (2023). Genetic analysis and QTL mapping of aroma volatile compounds in the apple progeny 'Fuji' × 'Cripps Pink.' Frontiers in Plant Science, 14, 1048846. https://doi.org/10.3389/fpls.2023.1048846
59. Yencho, G. C., Pecota, K. V., Schultheis, J. R., VanEsbroeck, Z. P., Holmes, G. J., Little, B. E., & Truong, V. D. (2008). 'Covington'sweetpotato. HortScience, 43(6), 1911–1914. https://doi.org/10.21273/hortsci.43.6.1911
60. Yao, Y., Zhang, R., Jia, R., Deng, Y., & Wang, Z. (2023). Impact of different cooking methods on the chemical profile of orange-fleshed sweet potato (Ipomoea batatas L.). Lwt, 173, 114288. https://doi.org/10.1016/j.lwt.2022.114288
61. Yu, X., Zhao, N., Li, H., Jie, Q., Zhai, H., He, S., Li, Q., & Liu, Q. (2014). Identification of QTLs for Starch Content in Sweetpotato (Ipomoea batatas (L.) Lam.). Journal of Integrative Agriculture, 13(2), 310–315. https://doi.org/10.1016/S2095-3119(13)60357-3
62. Yu, Y., Bai, J., Chen, C., Plotto, A., Yu, Q., Baldwin, E. A., & Gmitter, F. G. (2017). Identification of QTLs controlling aroma volatiles using a 'Fortune' x 'Murcott' (Citrus reticulata) population. BMC Genomics, 18(1), 646. https://doi.org/10.1186/s12864-017-4043-5
63. Zanor, M. I., Rambla, J. L., Chaïb, J., Steppa, A., Medina, A., Granell, A., & Causse, M. (2009). Metabolic characterization of loci affecting sensory attributes in tomato allows an assessment of the influence of the levels of primary metabolites and volatile organic contents. Journal of Experimental Botany, 60(7), 2139–2154. https://doi.org/10.1093/jxb/erp086
64. Zhang, R., Chen, H., Chen, Y., Tang, C., Jiang, B., & Wang, Z. (2023). Impact of different cooking methods on the flavor and chemical profile of yellow-fleshed table-stock sweetpotatoes (Ipomoea batatas L.). Food Chemistry: X, 17, 100542. https://doi.org/10.1016/j.fochx.2022.100542
65. Zhang, H., Dean, L., Wang, M. L., Dang, P., Lamb, M., & Chen, C. (2023). GWAS with principal component analysis identify QTLs associated with main peanut flavor-related traits. Frontiers in

Plant Science, 14, 1204415. https://doi.org/10.3389/fpls.2023.1204415

66. Zhang, J., He, L., Dong, J., Zhao, C., Wang, Y., Tang, R., Wang, W., Ji, Z., Cao, Q., Xie, H., Wu, Z., Li, R., Yuan, L., & Jia, X. (2023). Integrated metabolic and transcriptional analysis reveals the role of carotenoid cleavage dioxygenase 4 (IbCCD4) in carotenoid accumulation in sweetpotato tuberous roots. Biotechnology for Biofuels and Bioproducts, 16(1), 45. https://doi.org/10.1186/s13068-023-02299-y

67. Zhang, R., Tang, C., Jiang, B., Mo, X., & Wang, Z. (2021). Optimization of HS-SPME for GC-MS Analysis and its application in characterization of volatile compounds in Sweet potato. Molecules, 26(19), 5808. https://doi.org/10.3390/molecules26195808

68. Zhou, Y., Deng, R., Xu, X., & Yang, Z. (2020). Enzyme Catalytic Efficiencies and Relative Gene Expression Levels of (R)-Linalool Synthase and (S)-Linalool Synthase Determine the proportion of Linalool enantiomers in Camellia sinensis var. Sinensis. Journal of Agricultural and Food Chemistry, 68(37), 10109–10117. https://doi.org/10.1021/acs.jafc.0c04381

Figures

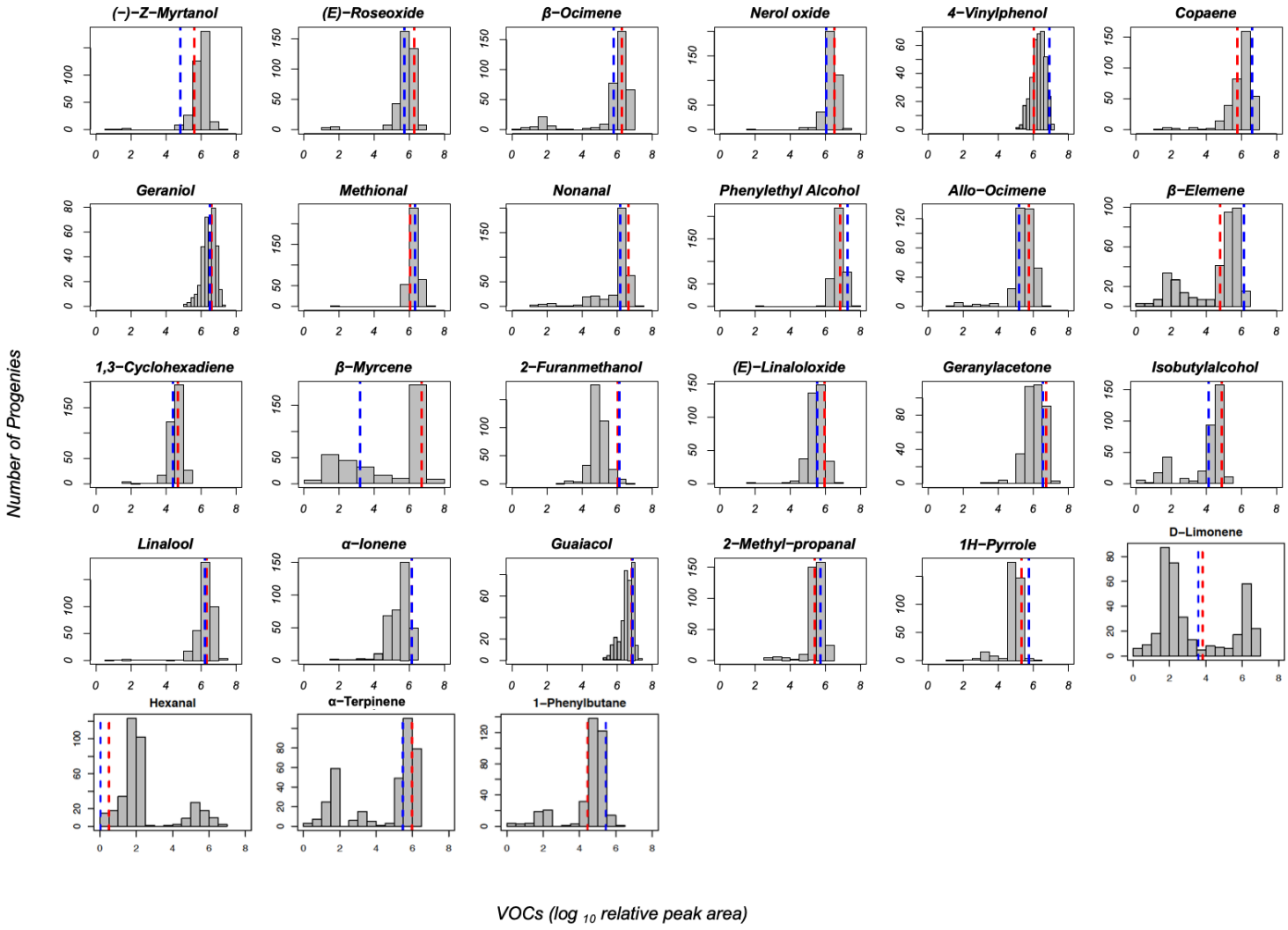


Figure 1

Frequency distribution of 27 flavor-associatedVOCs in the DC population. Gray bars represent the frequency of progeny for a given VOC abundance level, with the x-axis indicating the abundance of VOCs (log10 relative peak area) and the y-axis showing the number of progenies. Red and blue dashed lines indicate the parental values for “Covington” and “NCDM04-001,” respectively. The histograms illustrating the distributions of VOC abundance for the rest of the compounds are included in Fig S2.

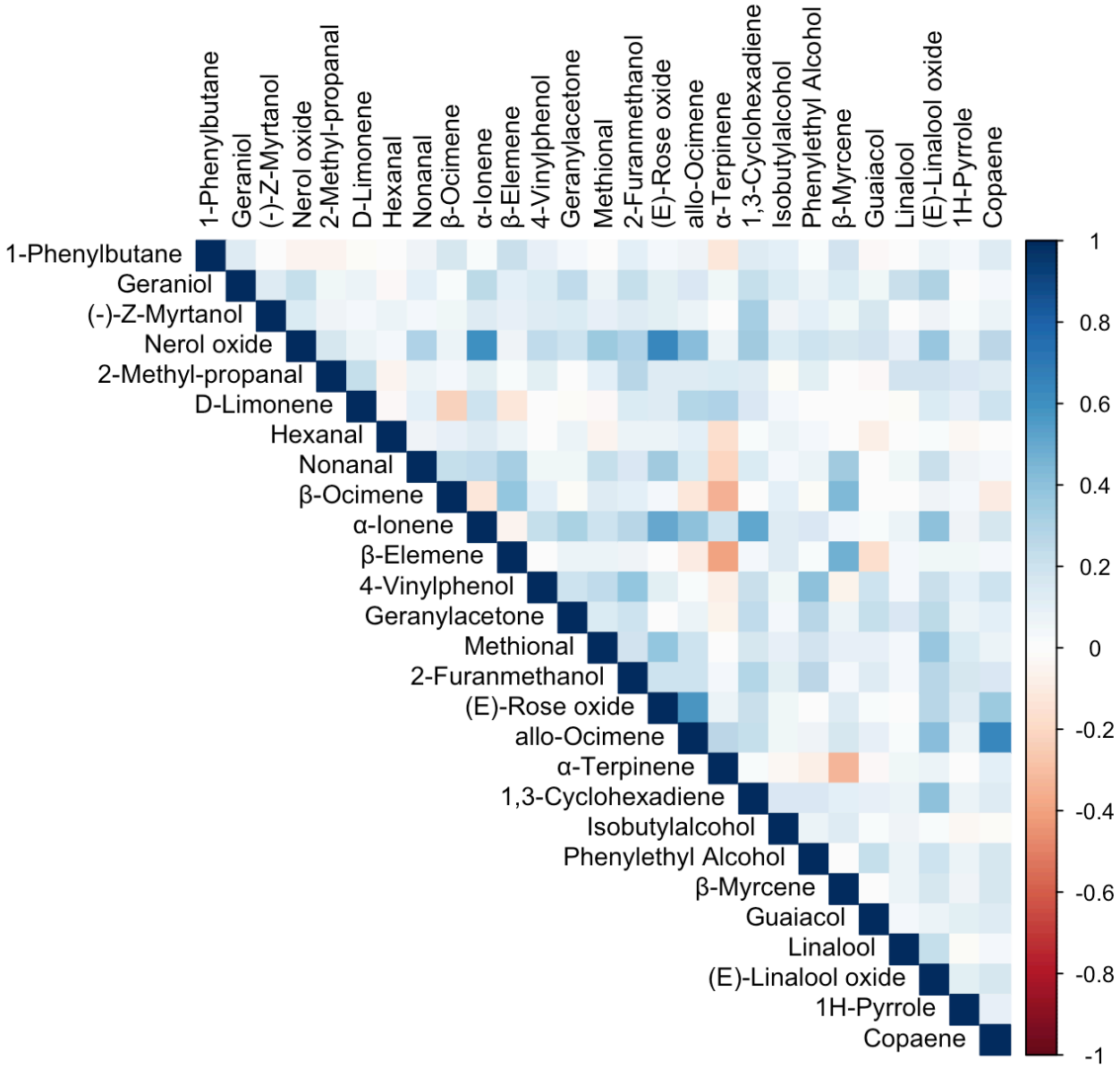


Figure 2

Correlation heatmap of 27 flavor-associated VOCs in the DC mapping population. Blue indicates a positive correlation and red indicates a negative correlation. The color intensity represents the strength of the correlation.

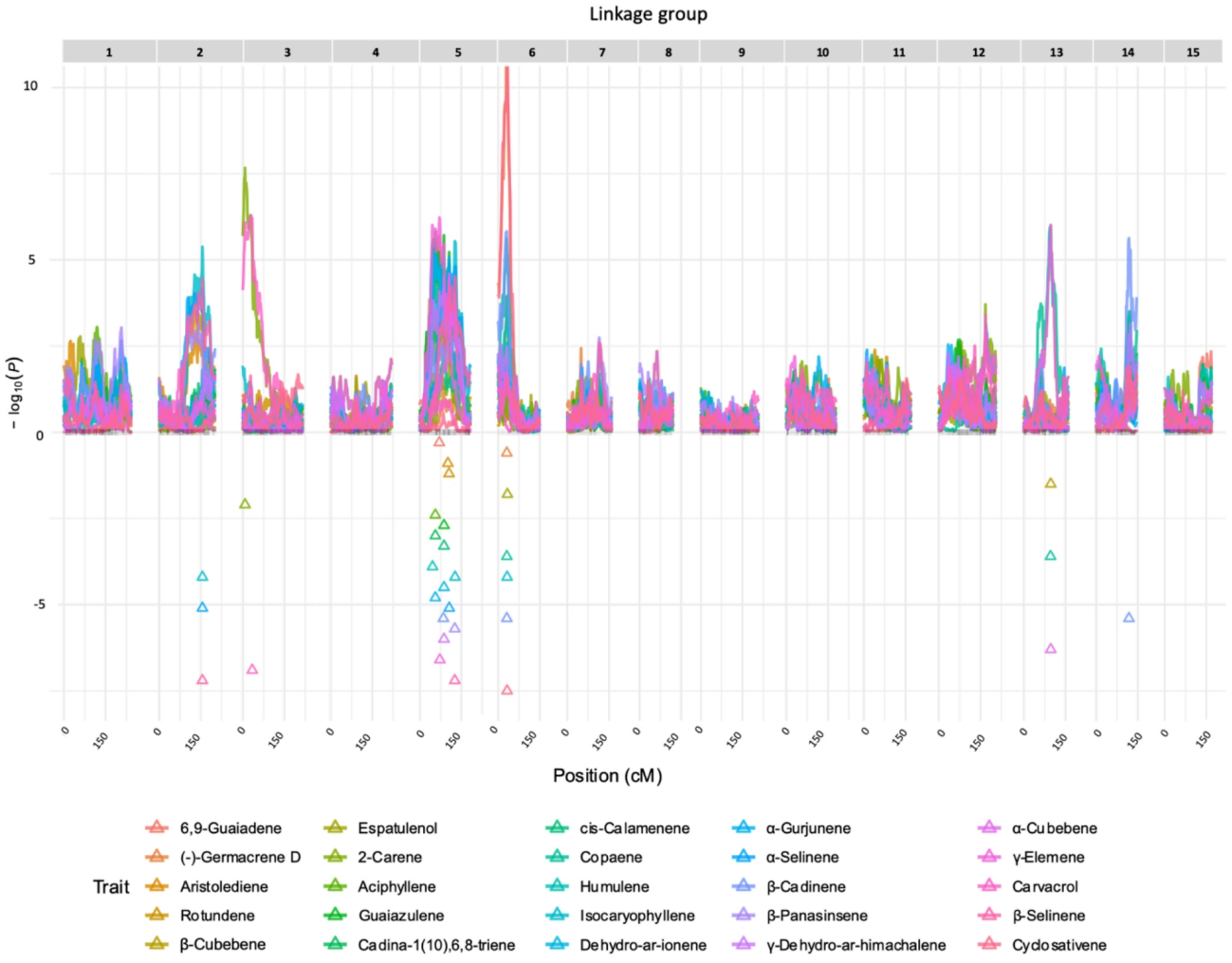


Figure 3

Plot showing the sesquiterpene QTLs in the DC population. -Log10(P) represents the logarithm of P values for every genomic position using the final QTL model for each trait.

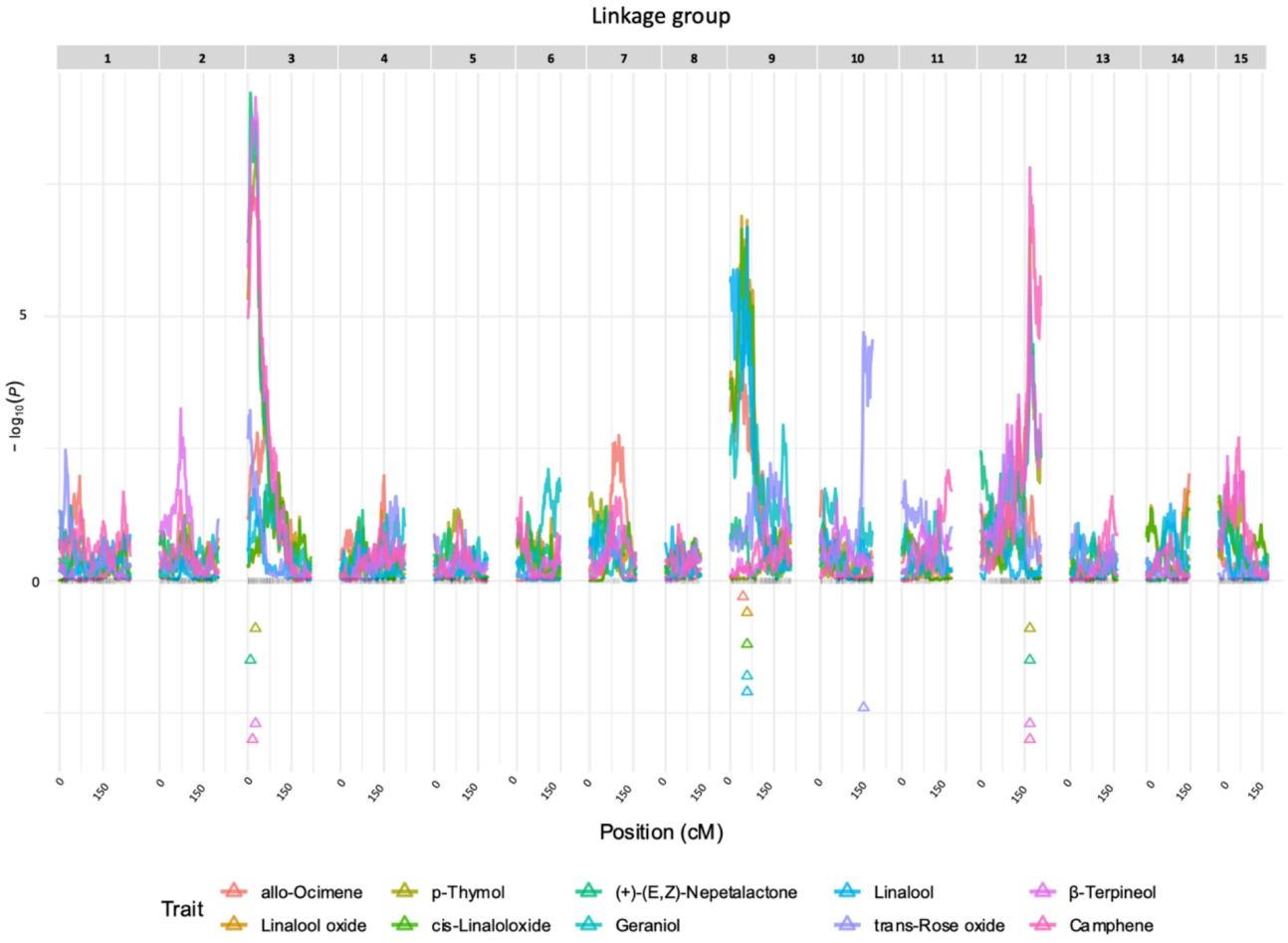


Figure 4

Plot showing the monoterpene QTLs in the DC population. -Log10(P) represents the logarithm of P values for every genomic position using the final QTL model for each trait.

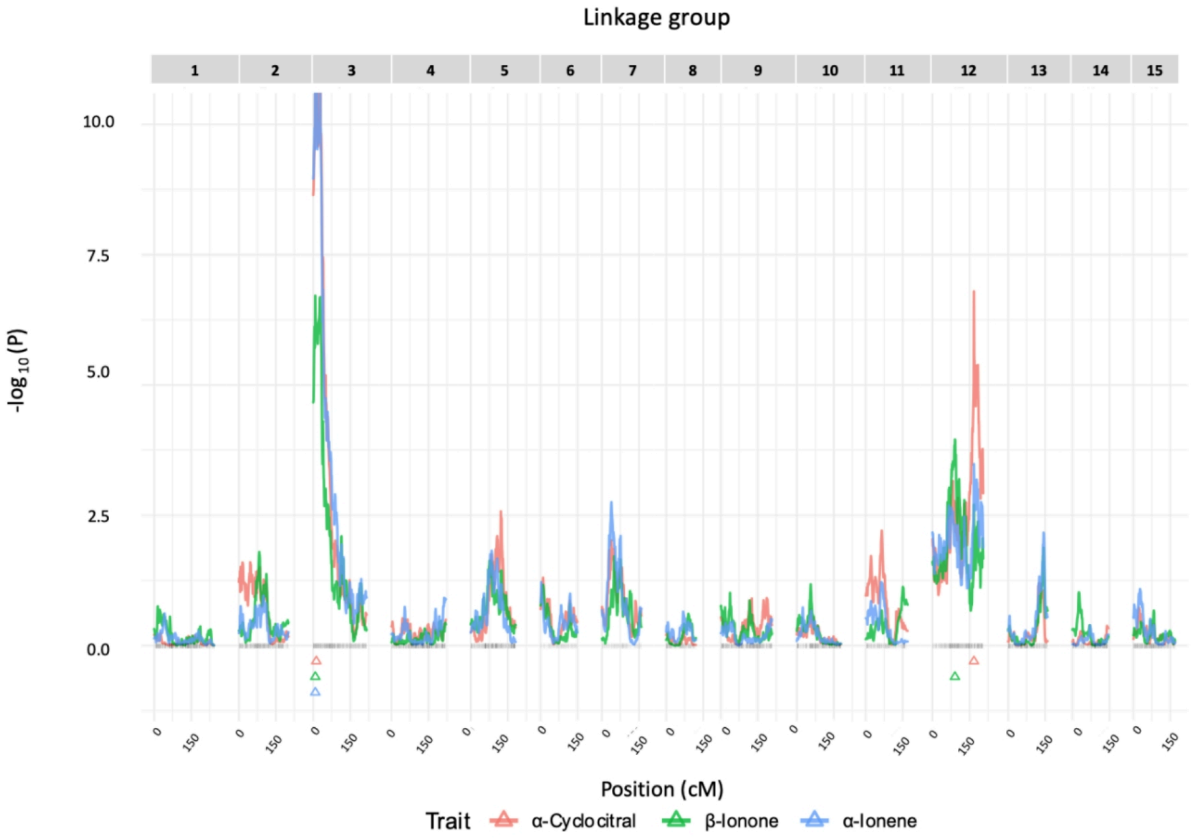


Figure 5

Plot showing the QTLs for apocarotenoids in the DC population. -Log10(P) is the logarithm of *P*values for every genomic position using the final QTL model for each trait. The ted dotted line represent the -Log10(P) significance threshold for the QTLs.

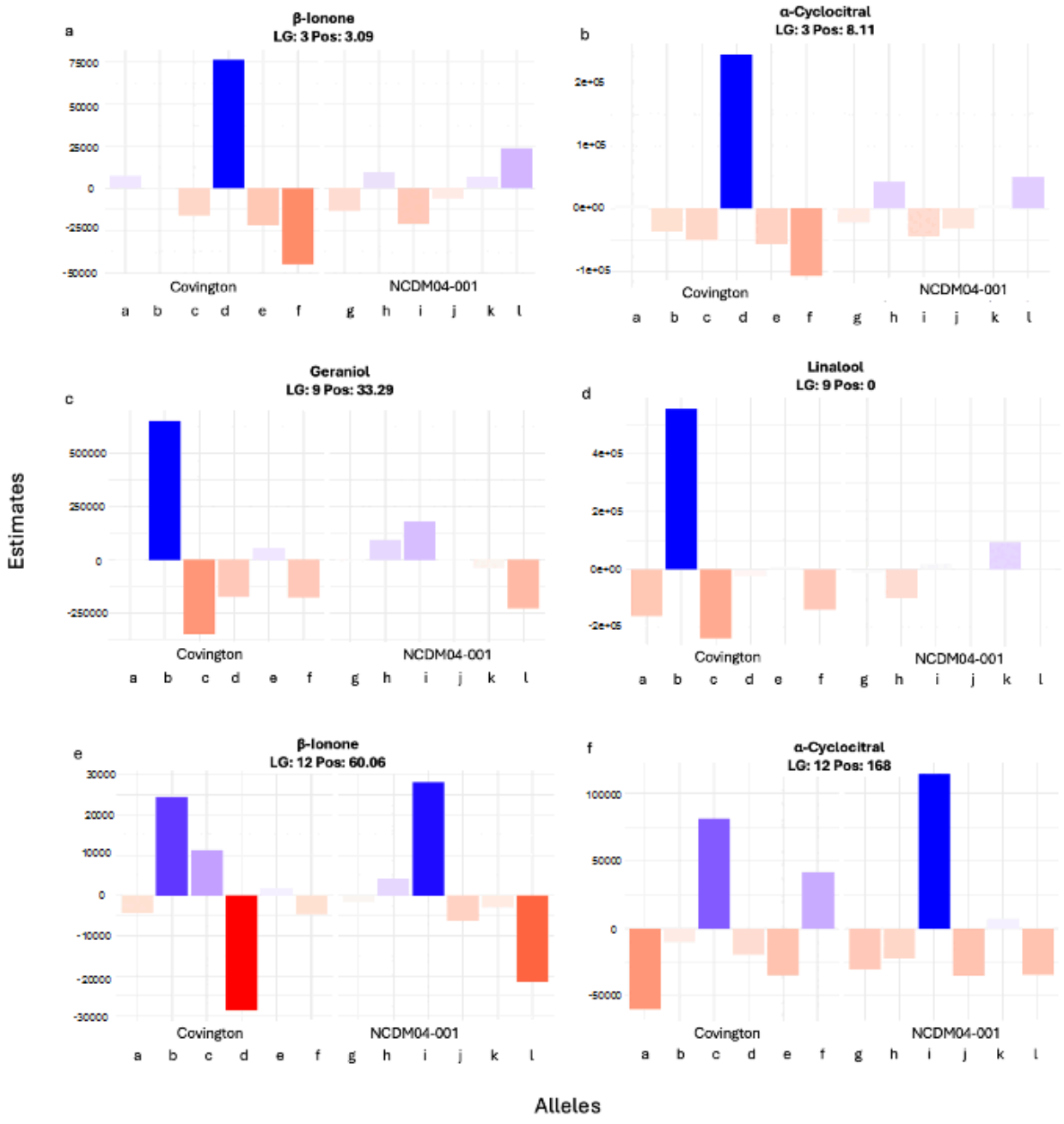


Figure 6

Representation of additive allelic effects for QTLs in LG 3, 9 and 12 derived from the parents, ‘Covington’ and ‘NCDM04-001’. Letters a through f and g through l represent the six haplotypes for QTLs derived from ‘Covington’ and ‘NCDM04-001’, respectively. Positive effects indicate an increased value for the traits, while negative effects indicate a decreased value for the trait.

Supplementary Files

This is a list of supplementary files associated with this preprint. Click to download.

- SupplementaryTablesVOCQTLAbugu.xlsx
- SupplementaryFiguresVOCQTLsAbugu.docx